

A Computational Fluid Dynamic Study of the Effects of a Synthetic Jet Actuator on an Airfoil

Arjav Anand Amur, Siddalingappa P. K.¹, S. Venkateswaran²

¹Associate Professor, ²Head of Department, Department of Aeronautical Engineering
Nitte Meenakshi Institute of Technology, Bangalore

Abstract - Flow separation is a phenomenon that occurs in almost all types of flows over aerodynamic bodies. Flow separations occur due to the effects of friction between the moving fluid and the surface, and adverse pressure gradients present within the boundary layer of the flow. Hence, separated flows are characterized by substantial energy losses, losses in lift and a significant increase in drag (pressure drag). For most practical applications in aerodynamics, the flow in boundary layers is predominantly turbulent. The objective of this project was to develop, implement, and analyse the effects of using a synthetic jet actuator, a zero - net - mass flux - active flow control technique, that 'actively' removes and injects air through a small cavity present on the flow boundary, to prevent, minimize, or completely eliminate the separation of the air flow over an airfoil, thereby improving the aerodynamic efficiency of the airfoil. Numerical simulations were performed with the actuator placed at 50 percent chord wise location along the NACA 0015 airfoil. Dynamic meshing was used to realistically simulate the reciprocating motion of the actuator.

Keywords – *Synthetic jet actuator, NACA 0015 airfoil, flow separation, active flow control technique, computational fluid dynamics.*

I. INTRODUCTION

Flow separation is a phenomenon that frequently occurs in all types of fluid - structure interactions. This phenomenon is often confused with the transition of boundary layers from a laminar to a turbulent one due to the similarities in the flow pattern, but is different in character and in the effects, it produces [1]. The frictional force between a fluid and a structure causes a retardation in their relative motion, affecting both the fluid and the structure [2]. The structure is subjected to a "tugging" force along the direction of the flow tangential to the structure's surface, called a shear force [2]. The reaction force due to the retardation on the fluid causes the local flow (fluid adjacent to the surface) velocity to decrease [2]. The flow velocity at the surface of the structure is zero [2]. This is called the no - slip condition [2]. The velocity of the flow increases in the normal direction to the surface, from zero to the freestream velocity. For the cases such as an airfoil, there is an increasing pressure gradient over the top surface as the flow moves towards the trailing edge. This is called an adverse pressure gradient. In addition to the retardation in relative motion due to frictional forces, the fluid close to the surface needs to work against the increasing pressure to move in the direction of the stream [2]. This further causes the velocity of the fluid to decrease [2]. As the fluid continues its journey downstream, it runs out of energy and comes to a stop ($V = 0$) [2]. Due to the adverse pressure gradient, the flow reverses causing large eddies (larger than the ones associated with a

turbulent boundary layer) to be formed [1]. This point at which the flow reverses is called the point of separation and the resulting eddies form a large wake of recirculating flow downstream of the surface also known as the 'dead air region' [1, 2]. Figure 1. illustrates the velocity profiles for such a flow phenomenon at different sections of a surface in the stream direction. Due to this separation, the pressure distribution is greatly altered and the flow now only sees a deformed 'effective body' [1, 2]. As a result, the fluid can no longer cancel the pressure generated on the lower surface and this leads to the production of drag called the pressure/form drag due to flow separation [1, 2]. In summary, the effects of flow separation include:

- Severe alteration of streamline flow.
- Substantial energy losses.
- Sudden loss of lift.
- Significant increase in drag (pressure/form).
- Violent unsteadiness in the flow resulting in buffeting of the body [1].

In comparison, turbulent boundary layers result in a higher velocity profile at the surface compared to a laminar one. This is largely due to the effective mixing of fluid particles from the outer regions resulting in higher energy fluid particles being pumped close to the surface [2]. Hence, a flow with a turbulent boundary layer is likely to separate later than one with a laminar boundary layer [1]. Modern flow control techniques exploit this fact to improve the aerodynamic efficiency of various fluid - structure interactions.

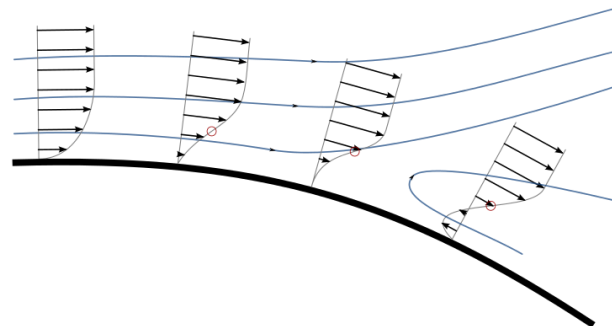


Figure 1: Velocity profiles for a separating flow at different sections of a surface in the stream direction.

Aerodynamic (or fluid) flow control is an emerging field of study that deals with changing the characteristics of flows, through external means to improve their aerodynamic

efficiency. Typical applications of flow control techniques include, mixing enhancement, drag reduction, lift augmentation and noise mitigation. Flow control techniques can be classified as active and passive techniques. Active flow separation control techniques are based on putting energy into the flow, while passive control techniques do not induce energy in the system. They only rely on changing the pattern of the flow to improve the efficiency of the flow. Some examples of active flow control techniques include:

1. Fluidic actuators - synthetic jet actuators
2. Moving object/surface actuators
3. Plasma actuators [3].

Some examples of passive flow control techniques include:

1. Vortex generators
2. Lift enhancing tabs [3].

II. SYNTHETIC JET ACTUATORS

A synthetic jet actuator is an active flow control device that intermittently removes and injects fluid through an orifice at a fixed rate. The synthetic jet actuator consists of an orifice at the surface of the fluid - structure boundary, a cavity, and a diaphragm/moving membrane fixed at the other end of the cavity. Figure 2. Illustrates a typical synthetic jet actuator. The frequency of the motion of the diaphragm defines the rate at which fluid is removed and injected. The fluid that is injected into the outer flow domain is in the form of a series of discrete vortical structures that 'synthesize' the jet [4].

One of the notable advantages of synthetic jet actuators is that the fluid required to create the jet is derived from the working fluid of the outer flow domain [4]. Since it transfers linear momentum to the flow - field without a net mass injection, it is often called the 'zero net mass flux' actuator [4, 9]. When the diaphragm expands, the fluid is sucked into the cavity causing the pressure inside the cavity to rapidly increase. In addition to the high-pressure gradient between the outer domain and the actuator cavity, on contraction of the diaphragm, the fluid is pushed out of the orifice, forcing the fluid to increase its velocity as it moves out. The flow then separates from the sharp edges of the orifice causing the fluid to form a circulating flow ultimately resulting in the formation of vortices [10]. A control system is utilized to maintain a time harmonic motion of the diaphragm [10]. Due to this, the shed vortex is not affected by the entrainment of fluid during the next cycle of suction and ejection of the actuator [10]. The vortices induced by the synthetic jet create a turbulent boundary layer on the fluid - surface interface of the flow on which it is employed, allowing the flow to remain energized through its journey along the surface of the structure, thereby delaying the separation by allowing the fluid to overcome the adverse pressure gradient. The net effect of this is an enhancement of the lift of the body and reduction in form drag.

The movement of the diaphragm (a flexible membrane) located inside the cavity maybe moved using a suitable mechanism [10]. For instance, a piston maybe positioned in a way such that the reciprocating motion of the piston moves the fluid in and out of the cavity [10]. Other suitable mechanisms include, using either a ceramic piezoelectric actuator which can alternately expand and contract the diaphragm when given

a sinusoidal voltage as the ceramic vibrates, or using a magnet surrounded by AC (alternating current) coils which lead to an alternating force being applied on the diaphragm in the presence of a magnetic field produced by the magnet [3, 10].

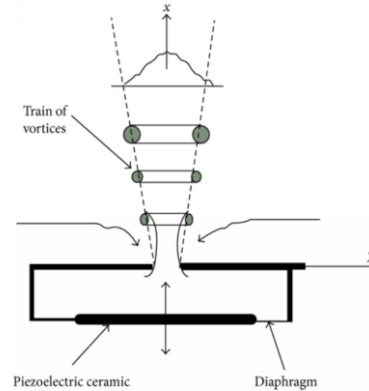


Figure 2: A typical synthetic jet actuator [5].

III. PARAMETRIC STUDIES AND EXPECTED RESULTS

For the synthetic jet actuator to be effective enough, a parametric study is vital, since the actuators are affected by parameters of the orifice, cavity and diaphragm [8]. In their paper, Jain et al. [8] have performed a detailed parametric study using numerical simulations of the various interlinked parameters of the synthetic jet. The various parameters varied by Jain et al. [8] include the orifice diameter, orifice height, shape of the orifice, cavity diameter, cavity height, frequency of the oscillations and the amplitude of the diaphragm. An increase in diaphragm amplitude results in an increased swept volume which causes more fluid to exit out of the orifice [8]. For larger amplitudes, the peak velocity is attained at a faster rate [8]. A phase angle is defined for the actuator cycle between the diaphragm position and the flow reversal at the orifice [8]. It was found that the phase angle increases linearly with an increase in the cavity height [8]. For smaller cavity heights, the velocity build up is held for a longer time while for larger cavity heights, the peak velocity is relatively lower as the diaphragm may reverse its motion by the time the velocity has built up causing a reduced pressure inside the cavity [8]. It is suggested that the phase angle should be less than 90° at any time to avoid adverse effects on the performance [8]. As the radius of the cavity directly determines the diaphragm height and hence the volume swept for a given amplitude, it was difficult to study the effects of this parameter without having to change the other parameters [8]. They demonstrated that by keeping the amplitude constant, the magnitude of the velocity decreased with a decrease in the swept volume and that by keeping the swept volume constant the amplitude varied exactly as predicted with a variation in the cavity radius [8]. They also found issues associated with small and large radius cavities in that - for a cavity with a small radius, the amplitude had to be higher to maintain the swept volume and hence because of the rapid acceleration of the diaphragm, the flow could not keep up with the diaphragm motion resulting lower peak velocities. In the case of larger cavity radii, the diaphragm did not cover the entire cavity height and therefore the pressure build up inside the cavity and the mass flow rate was relatively smaller [8]. The effects on the peak velocity due to changes in

the orifice height was negligible with a variation of about 4 m/s which accounted for a 14% change from the baseline case [8]. The size of the orifice diameter was varied from 1 mm to 8 mm [8]. The greatest velocity is obtained at 1 mm which seems to be intuitive [8]. For an actuator with an 8 mm orifice diameter, there is no jet as the fluid flowing out during the ejection stroke is sucked back in during the suction stroke [8]. Jain et al. [8] state that although a convergent orifice shape may help during the ejection stroke, during the suction stroke it might have a detrimental effect on the ejection velocity [8]. The fluid sees a diverging section which causes it to reduce its velocity leading to a decrease in mass flow and hence a diminution of the jet velocity [8]. The largest velocity reduces with a 1 mm orifice diameter up till 15° of nozzle angle [8]. Although higher ejection velocities were obtained beyond a nozzle angle of 15°, the peak velocity never can reach values obtained by normal straight orifices [8].

Most of the expected results for this project were obtained from the results of the simulations performed by Montazer et al. [6]. Montazer et al. displayed that optimal results in L/D ratios for a 13° angle of attack (the stall angle for the NACA 0015 airfoil) were obtained when the synthetic jet actuator was located between 24% - 36% of the chord from the leading edge, the orifice diameter was between 0.6 mm - 1.2 mm and the frequency of the diaphragm was between 60 Hz - 100 Hz [6]. The highest peak velocity obtained was 140 m/s and a percentage increase of 5.47% in the coefficient of lift was obtained for the above configurations [6]. The optimal results in L/D ratios for a 16° angle of attack was obtained when the location of the actuator was varied between 0.03% - 24% of the chord from the leading edge, the orifice diameter was between 0.6 mm - 1.2 mm and the frequency of the diaphragm was between 60 Hz - 90 Hz [6]. For these configurations, the highest peak velocity obtained was only 85 m/s and a percentage increase of 17.16% in the coefficient of lift was observed [6]. According to the authors, if the jet outflow is tangential to the external flow, the momentum boundary layer directly increases [6]. But if the jet outflow is normal to the external flow, the rate of mixing in the adjacent shear layer could increase [6].

IV. SIMULATION SETUP

The numerical simulation/CFD analysis of the problem involved recreating the required flow conditions in ANSYS Fluent for the model used in the experiment. A steady flow analysis was first run for the clean airfoil using the same physics setup to measure the point of separation, coefficients of lift and drag. A suitable mesh was later generated for the synthetic jet actuator integrated airfoil with the required number of nodes and elements spaced appropriately. A dynamic mesh was used to mimic the reciprocating motion of the diaphragm. Two different turbulence models were employed for the same case and the coefficients of lift, drag and pressure distributions over the synthetic jet actuator integrated models were solved for using a transient simulation. To ensure flow similarity, the same Reynold's number of 493013 (based on the chord length and the freestream velocity) was used for the simulation as used in the experiment.

A. Model Setup

The model was designed using the ANSYS Workbench DesignModeler software package. The coordinates for the NACA 0015 airfoil was obtained and was modified in excel into a form suitable for the current project (increased number of panels on the top and bottom surface, chord length of 180 mm, and a closed trailing edge). The far field was then drawn surrounding the airfoil. Parameters affecting the performance of the actuators such as the orifice diameter, orifice height, shape of the orifice, cavity diameter, cavity height, frequency of the oscillations and the amplitude of the diaphragm are listed in Table 1.

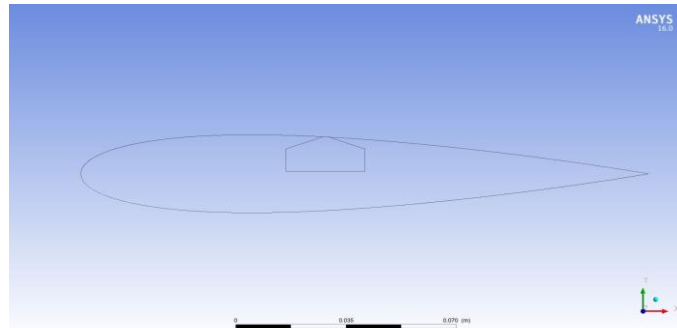


Figure 3: Synthetic jet actuator integrated model.

Parameter	Notation	Value	Units
Airfoil chord	c	180	millimeter
Amplitude	A	40	squared meter
Frequency	f	100	Hertz
Average phase angle	ϕ	20	degree
Cavity diameter	d _c	25	millimeter
Cavity height	h _c	8.3	millimeter
Orifice shape	-	Convergent	-
Orifice diameter	d _o	2	millimeter
Orifice height	h _o	4.15	Millimeter
Nozzle angle	θ	22.54	Degree
Location from trailing edge	x	90	millimeter
Far field length ahead	L ₁	2250	millimeter
Far field length behind	L ₂	2700	Millimeter

Table 1: Synthetic jet actuator design parameters.

B. Grid Generation

To get an acceptable accuracy for the solution a C - Grid type hybrid mesh was generated using the ANSYS Meshing software package. The mesh consisted of unstructured triangular elements throughout the grid with 30 layers of structured quadrilateral elements at the boundary of the airfoil. A total of 199495 elements with 157260 nodes were obtained.

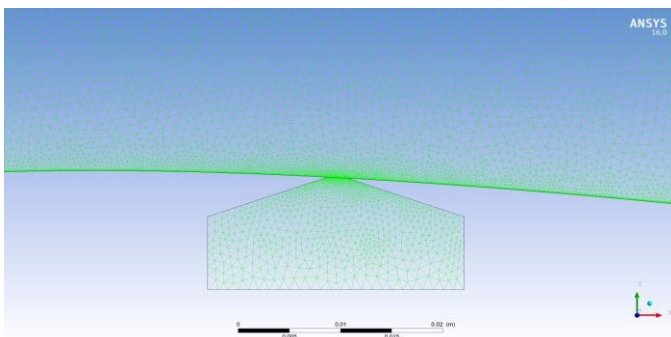


Figure 4: Mesh for the synthetic jet actuator.

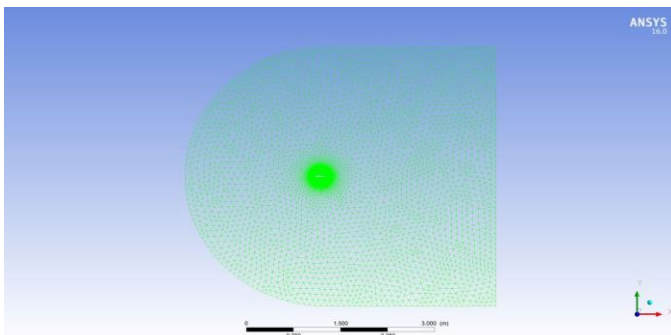


Figure 5: Mesh throughout the C-grid.

C. Dynamic Meshing

A dynamic mesh was used to realistically simulate the reciprocating motion of the actuator. A UDF (User Defined Function) was written to give the diaphragm a sinusoidal displacement in the Y - direction. In the commercial ANSYS Fluent software package, the Remeshing and Smoothing functions were applied to the actuator's mesh so that the mesh could deform without creating 'negative cell volume' errors.

D. Physics Setup and Numerical Solution

The ANSYS Fluent software package was used to setup the flow problem. The flow parameters were kept constant at standard sea level conditions (SSL), with a freestream velocity of 40 meters per second squared and a test angle of attack of 13 degrees. This results in a flow with a Reynold's number of 493013 and a Mach number of 0.117. Since the flow Mach number indicates that the flow is incompressible, the pressure based solver was selected. A transient simulation was necessary to get the diaphragm motion at different time intervals. For the viscous model, the near wall low Reynolds SST $k - \omega$ model was used to compute for the coefficient of lift, coefficient of drag and the pressure distribution over the airfoil. As already stated in the literature survey, the near wall low Reynolds SST $k - \omega$ turbulence model provides a satisfactory solution for separated flows over airfoils [7]. The LES (Large Eddy Simulation) turbulence model was used to obtain the turbulent kinetic energy contours to visualize the decrease in flow separation and the movement of the generated vortex. Under default settings in ANSYS Fluent, the LES turbulence model is generally deactivated. The command '(rpsetvar 'les-2d? #t)' is used to switch on the LES turbulence model. The material for fluids is selected as air and it has the required (SSL) Static Seal Level values as required. Under

Cell Zone Conditions, fluid is assigned to both the actuator and outer domain surface. The boundary conditions assigned to each part of the domain is tabulated in Table 2. The required reference values were computed from 'Far Field 1'.

Part Name	Boundary Condition
Far field 1	Velocity inlet
Far field 2	Pressure outlet
Fluid	Interior
Actuator fluid	Interior
Interface	Interior
Airfoil	Wall
Orifice wall	Wall
Cavity wall	Wall
Diaphragm	Wall

Table 2: Boundary conditions.

The coupled pressure - velocity coupling scheme was selected so that there was some control over the solution (parameters such as courant number and under relaxation factors could be changed) should divergence occur. A second order upwind scheme was used for the momentum, pressure, turbulent kinetic energy and specific dissipation rate variables. A second order implicit scheme was used for the transient formulation. A courant number of 1 and relaxation factors of 0.5 was specified for other variables as the solution diverged after a few iterations in the transient analysis. In addition to the residuals monitor, the coefficient of lift and drag monitors were activated and the values were set to produce averaged results for the entire flow time. The residuals were initially set to 1e-06 but as the solution diverged after a few iterations, the residuals were brought down to 1e-04 to make the solution more stable. A standard solution initialization was used and the initial values were computed from 'Far Field 1'. The time step size for the transient solution was given as 0.1 second and the total number of time steps as 90 producing a total flow time of 9 seconds. The number of iterations for each time step was set at 10 to get a reasonable computational time.

V. RESULTS

The solution yields a time averaged coefficient of lift, and coefficient of drag value for the synthetic jet actuator integrated airfoil, for a total of 9 flow seconds. These values are compared to the values obtained for the clean airfoil using the same mesh, flow physics and solver settings and are validated using the values obtained by the authors of reference [6]. Table 3. Shows the comparison and the percentage increase/decrease in these values.

Coefficient	Clean	With Synthetic Jet	Percentage Change
Lift	1.0978	1.1196	2 %
Drag	0.0969	0.0838	7.64 %

Table 3: Comparison of coefficients for clean and integrated airfoils.

We see that there is a reasonable percentage increase in the coefficient of lift and decrease in the coefficient of drag. However, in comparison to the values obtained by simulations performed by other authors (for example reference [6]), these values are still low. This can be accounted for the unstructured triangular mesh employed and size of the residuals used. With

a finer structured mesh, close to the airfoil surface, we might be able to get a better solution and a lower percentage error for the coefficients.

From the LES turbulence model computation, we can get a clearer picture of the buildup of the vortex at the exit of the orifice and at the surface just adjacent to the orifice. The maximum velocity obtained by using the near wall low Reynold's number $k - \omega$ turbulence model is 88.91 square meter. Figures 6., 7., and 8. show the development of this vortex at the orifice exit. Figure 9. shows the fully developed vortex adjacent to the vortex formed due to flow separation close to the trailing edge of the airfoil. Figure 10. shows the comparison between the velocity contours of the flow over the clean airfoil and the actuator integrated airfoil.

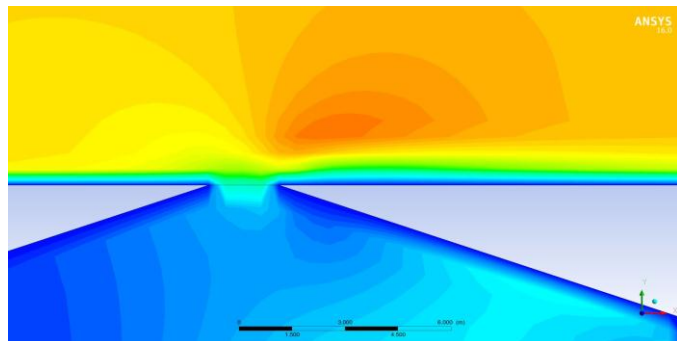


Figure 6: Vortex at $T/3$.

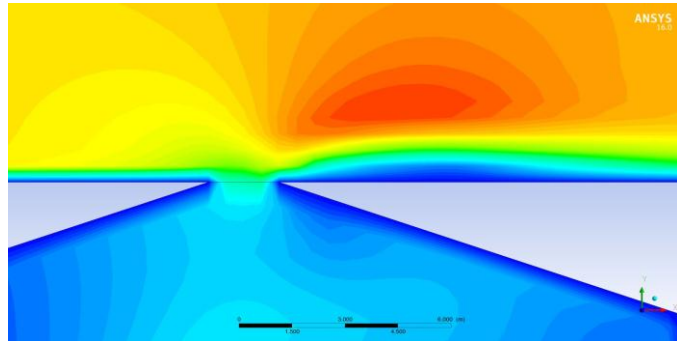


Figure 7: Vortex at $2T/3$.

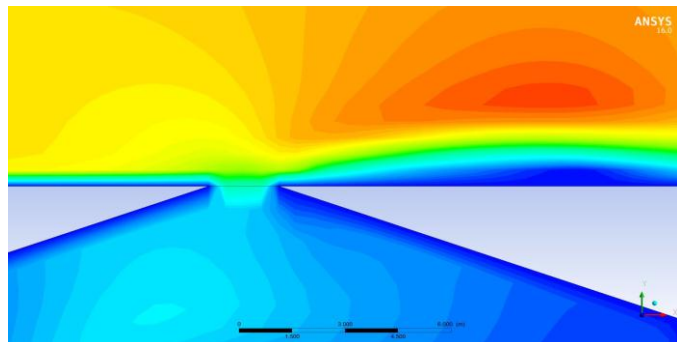


Figure 8: Vortex at T .

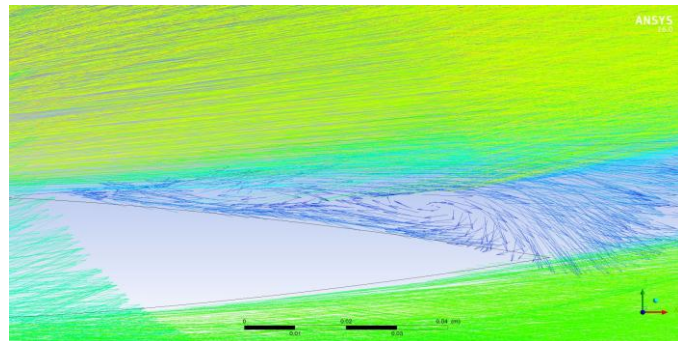


Figure 9: Vector map for synthetic jet actuator integrated airfoil.

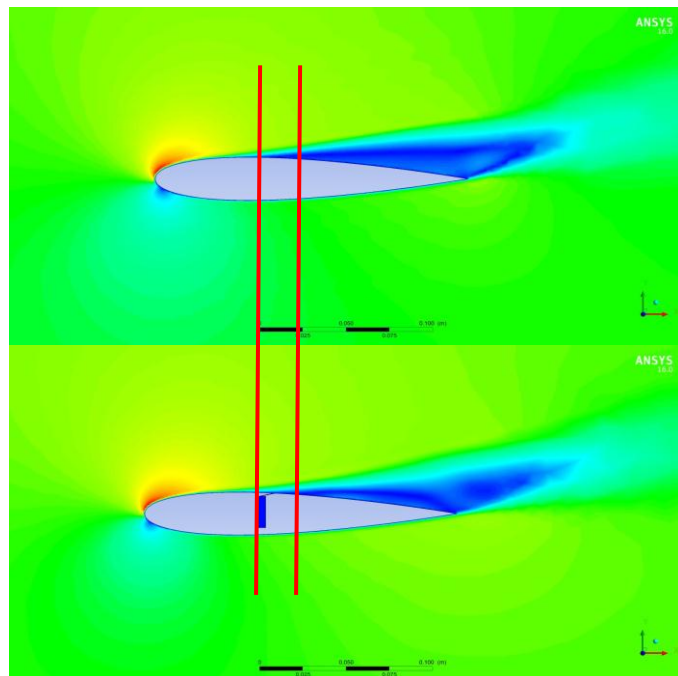


Figure 10: Comparison of the velocity contours for a clean airfoil and the actuator integrated airfoil showing the delay in flow separation. (Note: Pictures used for comparison of the airfoils make use of a synthetic jet actuator of different shape but produce the exact same results as the current shape used in this paper).

In conclusion, we see that by using a synthetic jet actuator, the aerodynamic efficiency of any structure can be significantly increased by delaying the point of separation of the flow over the body. We also find that due to a suction effect created by the actuator, the pressure drag created by the body decreases by a reasonable value. Although an increase in lift was obtained, with further refinement of the numerical methods used and an optimization of the actuator dimensions through a detailed parametric study, can yield a higher percentage increase in lift.

ACKNOWLEDGMENT

We would like to thank our college Nitte Meenakshi Institute of Technology, Bangalore, for giving us the opportunity to work on this project and providing us with the necessary support in the form of laboratory time and licensed software.

REFERENCES

- [1] Clancy, L.J., *Aerodynamics*.
- [2] D. Anderson Jr., John, *Fundamentals of Aerodynamics*, McGraw Hill 2010 (5th Edition).
- [3] Jansen, D.P., *Passive Flow Separation Control on an Airfoil - Flap Model - The Effect of Cylinders and Vortex Generators*, Master of Science Thesis, August 2012.
- [4] Glezer, Ari, *Some Aspects of Aerodynamic Flow Control Using Synthetic - Jet Actuation*, Philosophical Transactions of the Royal Society A, 2011.
- [5] Li, Hua, Villanueva, Walter & Kudinov, Pavel, *Approach and Development of Effective Models for Simulation of the Thermal Stratification and Mixing Induced by Steam Injection into a Large Pool of water*, Hindawi Publishing Corporation, Science and Technology of Nuclear Installations, Volume 14, July 2014.
- [6] Montazer, E., Mirzaei, M., Salami, E., Ward, T.A., Romli, F.I., & Kazi, S.N., *Optimization of a Synthetic Jet Actuator for Flow Control Around and Airfoil*, IOP Publishing, IOP Conference Series: Materials Science and Engineering 152, 2016.
- [7] Duvigneau, Regis & Visonneau, Michel, *Optimization of a Synthetic Jet Actuator for Aerodynamic Stall Control*, Laboratoire de Mecanique des Fluides, Ecole Centrale de Nantes.
- [8] Jain, Manu, Puranik, Bhalchandra & Agrawal, Amit, *A Numerical Investigation of Effects of Cavity and Orifice Parameters on the Characteristics of a Synthetic Jet Flow*, Sensors and Actuators A: Physical, Elsevier B.V., 2010.
- [9] Saambavi, Karunakaran, *Flow Separation Control Using Synthetic Jets on a Flat Plate*, Master of Science Thesis, April 2014.
- [10] *Synthetic Jet Actuator and Their Applications*, US Patent, US 5758823, June 1998.